Available online at www.sciencedirect.com
SCIENCE DIRECT
Remote Sensing of Environment 102 (2006) 377–389
Remote Sensing of Environment
www.elsevier.com/locate/rse

SMOSREX: A long term field campaign experiment for soil moisture and land surface processes remote sensing

Patricia de Rosnay [a,*], Jean-Christophe Calvet [b], Yann Kerr [a], Jean-Pierre Wigneron [c], François Lemaître [d], Maria José Escorihuela [a], J. Muñoz Sabater [b], Kauzar Saleh [c], Joël Barrié [b], Gilles Bouhours [b], Laurent Coret [a], Guy Cherel [b], Gérard Dedieu [a], Roger Durbe [b], Nour Ed Dine Fritz [b], Francis Froissard [b], Joost Hoedjes [a], Alain Kruszewski [c], François Lavenu [a], David Suquia [b], Philippe Waldteufel [e]

[a] *CESBIO (Centre d'Etudes Spatiales de la BIOsphère), UMR5126 CNES/CNRS/IRD/UPS, BPI 2801, 18 ave Edouard Belin, 31401 Toulouse cedex 9, France*
[b] *Météo-France, CNRM/GAME, URA CNRS 1357, France*
[c] *INRA (Institut National de Recherche Agronomiques) EPHYSE, Bordeaux, France*
[d] *ONERA (Office National d'Etudes et de Recherches Aérospatiales), France*
[e] *IPSL/SA (Institut Pierre Simon Laplace/Service Aéronomie, France*

Received 25 October 2005; received in revised form 15 February 2006; accepted 18 February 2006

Abstract

The primary goal of the SMOS mission is to deliver global fields of sea surface salinity and surface soil moisture using L-band (1.4 GHz) radiometry. Within the context of the preparation of SMOS activities over land, a field campaign, SMOSREX (Surface Monitoring Of the Soil Reservoir EXperiment), has been in operation since January 2001 in Mauzac, near Toulouse in France. Continuous ground measurements of meteorological variables, soil moisture and temperature profiles have been taken over bare soil and a grass plot left fallow. Since January 2003, SMOSREX has been providing accurate field measurements of dual polarized L-band brightness temperature up-welling from both bare soil and fallow plots, together with multi-spectral (from visible to infrared frequencies) remote sensing surface data. The scientific objectives are presented in this paper and the corresponding experimental design is described. The experimental concept is totally new since (i) SMOSREX combines land–surface–atmosphere observations, passive microwave measurements and VIS to NIR remote sensing, (ii) SMOSREX is based on highly accurate L-band measurements carried out by a radiometer specifically designed for the experiment, and (iii) SMOSREX provides a unique continuous data set of L-band measurements over several years. The characteristics of the L-band emission are presented at diurnal, seasonal and annual temporal scales, and the emissions are compared over bare soil and natural grass. The surface emissions over bare soil and fallow area are shown to be counter-phased at the diurnal scale due to small variations in vegetation water content and bare soil surface moisture. Innovative long term results using L-band measurements for both bare soil and natural grass are presented in this paper, and the relationship between the surface emission at L-band and surface bare soil moisture is shown to be suitable for a long term period (19 months). Soil freezing is shown to be drastically different for bare soil and vegetation covered plots, with a large threshold effect on microwave surface emission.
© 2006 Elsevier Inc. All rights reserved.

Keywords: Field campaign; Soil moisture; Remote sensing; L-band radiometry; Land surface processes

1. Introduction

Soil moisture is a key variable that characterizes the interface between continental surfaces and the atmosphere. It controls the partitioning of water and energy fluxes at the Earth's surface, and plays a critical role on the continental water distribution through land–surface–atmosphere feedback mechanisms. Soil moisture also affects land-use and agricultural planning, and is of major importance for many interrelated disciplines such as weather forecasting and hydrology (Entekhabi et al., 1999; Koster et al., 2004).

* Corresponding author. Tel.: +33 5 61 55 85 24; fax: +33 5 61 55 85 00.
E-mail address: patricia.derosnay@cesbio.cnes.fr (P. de Rosnay).

0034-4257/$ - see front matter © 2006 Elsevier Inc. All rights reserved.
doi:10.1016/j.rse.2006.02.021

Microwave technology has demonstrated a quantitative ability to measure soil moisture under a variety of topographic and vegetation cover conditions and it has proven to be suitable for satellite systems. Within this context, the Advanced Microwave Scanning Radiometer (AMSR-E) on the Earth Observing System (EOS) Aqua satellite was launched in May, 2002. It measures radiation at six frequencies in the range 6.9–89 GHz, and provides soil moisture estimates with a global coverage (Njoku et al., 2003). The SMOS (Soil Moisture and Ocean Salinity) mission is scheduled for launch in 2007 and the goal over continental surfaces is to deliver global fields of surface soil moisture using L-band radiometry (Kerr et al., 2001). The Hydrosphere State Mission (Hydros), project aims at combining radar and radiometer systems (Entekhabi et al., 2004).

In terms of preparing the SMOS mission, SMOSREX (Surface Monitoring Of the Soil Reservoir EXperiment) aims at improving microwave radiative modeling of soil–vegetation systems as well as improving the understanding of soil–plant–atmosphere interactions. SMOSREX is comprised of three components: (i) multi-frequency remote sensing in the solar to thermal infrared domains and L-band radiometry, (ii) a comprehensive set of ground measurements: vegetation and soil, meteorology, land surface fluxes, and (iii) both radiative transfer and land surface models. The objectives of this campaign are to (i) contribute to a better understanding of the different processes affecting the microwave signal, including specific events such as rainfall interception, dew deposition, or soil and vegetation freezing, (ii) test and improve the soil moisture retrieval algorithms from dual polarized and multi-angular measurements, and (iii) to develop the multi-frequency assimilation of remotely sensed surface variables in land surface models.

SMOSREX began in 2001 with ground measurements, and it was expanded in 2003 to include multi-spectral remote sensing measurements. By the end of 2006, SMOSREX will have provided a four-year data set of L-band multi-angular, dual polarized brightness temperatures, together with a complete set of meteorological, soil and vegetation, ground and remotely sensed measurements.

A number of previous L-band radiometry studies were devoted to passive microwave measurements of the surface either at the field scale (Choudhury et al., 1979; De Jeu et al., 2004; Eagleman & Lin, 1976; Schneeberger et al., 2004; Wang & Choudhury, 1981; Wigneron et al., 2002, 1996, 2004) or at larger scales using aircraft measurements (Bindlish et al., in press; Jackson et al., 1999, 1995; Schmugge et al., 1992). After almost 30 years of research, the relationship between soil moisture and microwave emission of the surface has been clearly shown to be significant for a large range of soil types and crop covers. In all of these experiments, however, microwave measurements were of limited duration (a couple of months at most), preventing the study of the long term stability of microwave algorithms. However, for satellite applications, the long term stability of microwave algorithms is critical. SMOSREX allows the consideration of microwave radiometry on inter-annual scales, and it enables the consideration of low frequency processes (vegetation cycle at annual and inter-annual scales) as well as the monitoring of specific infrequent events (soil freezing, soil roughness modifications, mowing of the grass). Accordingly, it opens the possibility for improvement, testing and validation of microwave modeling and retrieval algorithms for long time periods, including a large range of soil water content, vegetation and meteorological conditions. This is essential for improving the understanding of microwave radiometry in a complex medium such as soil–vegetation systems, as well as on the development of stable algorithms for future satellite applications.

A large number of studies, to investigate multi-temporal scale effects of water interception, soil roughness, freezing and effective soil temperature on L-band emission of the surface, as well as soil moisture retrievals, litter modeling, assimilation in land surface models, will be based on SMOSREX. The aim of the present paper is not to investigate in depth any of this particular issue; rather, it presents an overview of the scientific objectives of the experiment in these different fields by showing the first results of SMOSREX which are very new in terms of accuracy of the microwave measurements, the multi-temporal scale and the contrasted land cover types considered.

The next section presents the experimental design of SMOSREX. Section 3 shows some SMOSREX results. In Section 3.1, the processes that govern vegetation water content variability are shown and multi-spectral remote sensing is shown to be suitable to quantify the biomass of natural grass. Section 3.2 shows the effect of rainfall on the multi-angular remotely sensed brightness temperatures at 1.4 GHz, on both bare soil and natural grass. In Section 3.3, the surface emission diurnal cycle is investigated for these two types of surfaces. Section 3.3 focuses on soil and vegetation freezing effects, while Section 3.4 shows long term results at the annual scale for the fallow and the bare soil areas. Section 4 concludes and introduces the broad range of scientific investigations opened by this innovative long term field experiment for multi-frequency remote sensing of land surfaces.

2. Field and experiment description

The SMOSREX field site is located on the ONERA complex (Office National d'Etudes et de Recherches Aérospatiales) near the town of Mauzac (43°23′N, 1°17′E, at 188 m altitude), south of Toulouse (France), close to the Garonne River. Fig. 1 shows a schematic map of the site. It consists in two plots, the extension of which is indicated in Fig. 1: in the northern part of the site, the soil is kept bare, while the southern part of the site is covered by vegetation (natural fallow). The remote sensing instruments are installed at the top of the central structure, 15 m above the ground. The L-band radiometer (LEWIS) field of view, corresponding to 13.5° beamwidth, is reported for each incidence angle between 20° and 60°, according to values indicated in Table 1. SMOSREX began in January 2001 with ground monitoring of land surface processes. The ground installation, similar to that of MUREX conducted from 1995 to 1998 (Calvet et al., 1999), includes ground measurements of meteorology, heat

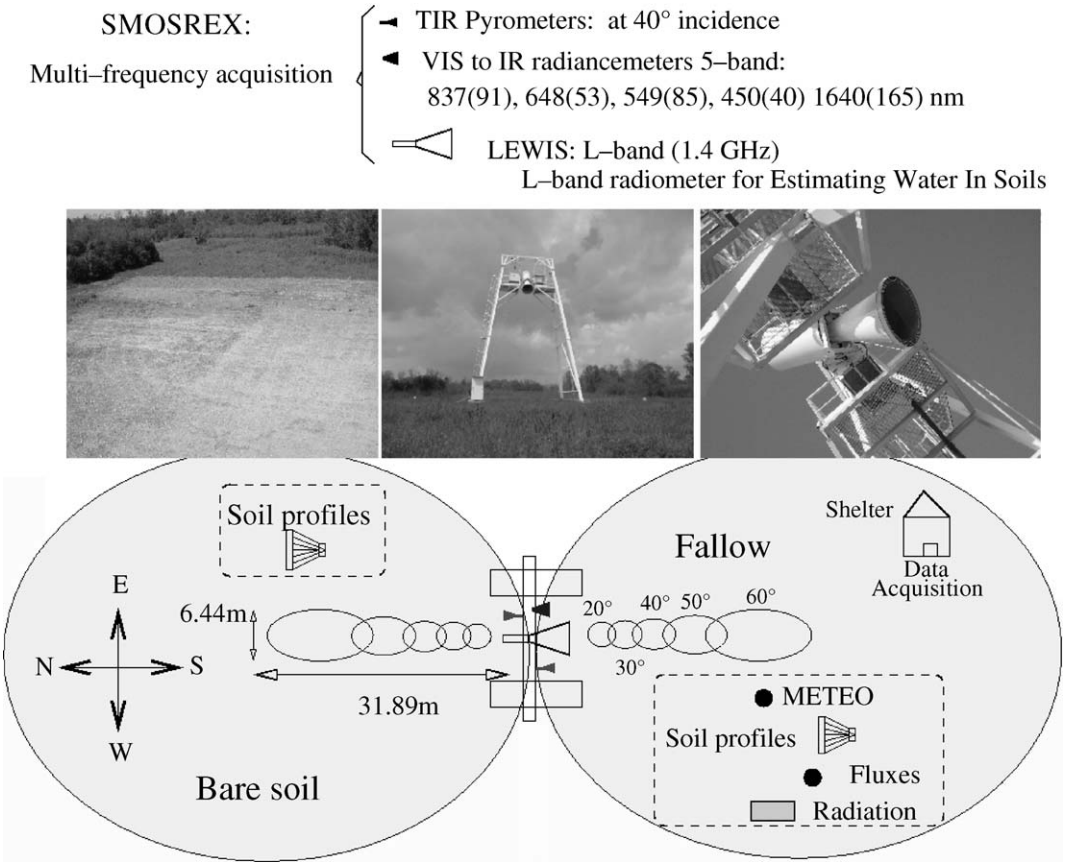

Fig. 1. Global map of the SMOSREX field site.

fluxes, moisture and temperature profiles in the soil, as well as soil texture, gravimetric and biomass measurements. In January 2003, the complete experiment started with the implementation of the remote sensing instrumentation, consisting of multi-spectral observation of the surfaces, in visible and thermal infrared domains and in microwave with L-band radiometer LEWIS described later in Section 2.2. SMOSREX is expected to last at least four years with remote sensing measurements until the end of 2006. Fig. 2 summarizes the chronology of the SMOSREX experiment deployment.

Fig. 3 depicts the annual cycles, monitored for SMOSREX field site, of both precipitation and air temperature from January 2001 to the end of August 2004. It shows that the weather conditions near Toulouse are generally well contrasted with a dry-hot summer and humid-cool winter. Associated annual cycles of vegetation are also very contrasted as shown on Fig. 4. Fallow is mowed every year in February. Besides the contrasted annual cycles, these figures point out the strong inter-annual variability of the climate conditions and interacting vegetation. Annual values of precipitation were 621,677, 574 and 634 mm in 2001, 2002, 2003 and 2004, respectively. The summer of 2002 experienced a large amount of rainfall and was characterized by dense vegetation from July to September. In contrast, for both 2003 and 2004, dry summer conditions lead to contrasting annual cycles, with vegetation indexes reduced to zero in August. A dry spring in 2003 inhibited optimum vegetation development, while a particularly rainy spring in 2004 resulted in significant vegetation growth in April–May. The 2003 and 2004 data also include simultaneous multi-spectral remote sensing measurements. In this paper we will therefore focus on these two years because they are particularly relevant for SMOSREX.

Table 1
Dimensions and position of the LEWIS Field of View (FOV) for different incidence angles

Incidence angle (°)	FOV length (m) (North–South)	FOV width (m) (East–West)	FOV area (m^2)	Distance from structure (m)	
				Max	Min
20	3.69	3.427	9.93	6.91	3.22
30	4.34	3.72	12.68	10.23	5.89
40	5.58	4.2	18.41	14.56	8.98
50	8.01	5.01	31.52	20.9	12.89
60	13.54	6.44	68.48	31.89	18.35

These characteristics correspond to 13.5° beamwidth (−3 dB) of a focal point located 13.7 m above the ground, according to LEWIS position on the structure.

2.1. Ground measurements

2.1.1. Meteorology

A weather station performs continuous half-hourly measurements of precipitation, 2 m air temperature and air humidity, 10 m wind speed and direction, atmospheric pressure, solar and atmospheric incoming radiation. Land surface fluxes (sensible

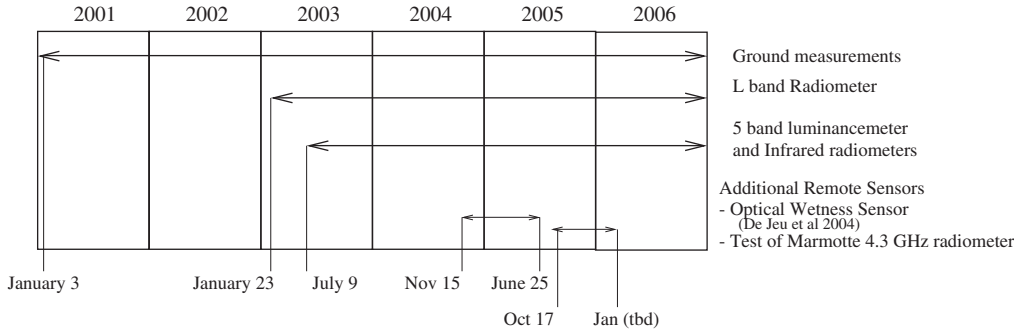

Fig. 2. Calendar of ground based and remote sensing instrumental deployment during the SMOSREX field experiment.

and latent heat fluxes) are also estimated above the fallow area in view of land surface model validation. These atmospheric measurements are used to understand the interaction processes between soil, vegetation and atmosphere and their direct and indirect influences on the remotely sensed signals at different frequencies.

2.1.2. Soil moisture and temperature

Soil moisture profiles are automatically measured at a 30-min time step by impedance sensors (ML2 Theta-probes[1]) installed at the following depths: 0–6 cm (×4), 10 cm (×3), 20 cm (×3), 30 cm (×2), 40 cm (×2), 50 cm (×2), 60 cm (×2), 70 cm, 80 cm, 90 cm. Sensors are duplicated at each depth from 0 to 60 cm in order to improve the sampling in the near-surface soil layers where higher levels of spatial and temporal variability of soil moisture are observed. Soil temperatures are measured at 1, 5, 20, 50 and 90 cm by thermistor probes. Soil profile measurements and protocols are identical on fallow area and bare soil. Gravimetric measurements were regularly performed in a large range of soil moisture conditions for calibration of the soil moisture sensors on both plots.

2.1.3. Soil texture and roughness

Surface textural class is loam with 16.6% and 15.6% clay, 47.4% and 47.2% silt, 36.0% and 37.2% sand for the bare soil area and the fallow area respectively. At depth, the soil texture of the bare soil area gets more sandy while the texture profile gets more fine textured underneath the fallow area. The soil roughness influences the L-band emission of the soil surface (Choudhury et al., 1979; Ulaby et al., 1982; Wang, 1983). It was measured, on both fallow area and bare soil using a pine profiler, 2 m long with 201 needles. The roughness of the soil underneath the natural grass is found to be stable for the experiment duration. The rms (root mean square) height, s, is estimated to be constant at 7.06 mm with a standard deviation (sd) of 0.98 mm, and the correlation length is lc = 101.13 mm (sd 28.6 mm). Bare soil is more exposed to the atmosphere and may be affected by meteorological conditions. Its surface roughness was measured in July 2003 (during a drought), in February 2004 (following several strong precipitation and soil freezing events), and again in April 2004. The obtained values for the rms height s (and standard deviation) were, respectively, 11.26 mm (2.5 mm), 11.09 mm (3.6 mm) and 9.12 mm (2.18 mm). The correlation lengths (and sd) were, respectively, 65.26 mm (32.93 mm) in July, 2003, 101.2 mm (42.2 mm) in February, 2004, and 70.7 mm (33.71 mm) in April 2004. The bare soil field was ploughed in November 2003. Then the soil roughness decreased slowly for several months. This decrease of soil roughness is captured by February and April measurements.

2.1.4. Vegetation

The measurements of the vegetation characteristics (height, biomass, dry matter, water content and LAI) were performed frequently during spring, summer and fall, with sparser measurements being taken in winter when vegetation phenology is slower. Samples area of 25×25 cm^2 area were randomly chosen in the fallow area next to the LEWIS radiometer field of view in order to measure vegetation mass and water content using a fresh and dry weighing method. For each sample, green biomass and dead plant material were measured separately. For green biomass, the LAI measurements were performed during 2001, 2002, 2003 and 2004 (Fig. 4).

2.2. The L-band radiometer LEWIS

L-band microwave measurements are performed by LEWIS (L-band radiometer for Estimating Water In Soils). LEWIS is equipped with a Potter horn antenna (ensuring very low side-lobe levels) and it measures brightness temperature at the L-band (1.4 GHz) for both horizontal and vertical polarizations. The LEWIS beamwidth is 13.5° at -3 dB and its accuracy is 0.2 K. Lemaître et al. (2004) give a full description of the LEWIS radiometer (Lemaître et al., 2004). Data have been automatically monitored by LEWIS since January 23, 2003, with a 6 s time step. LEWIS is installed at the top of a 15 m structure (Fig. 1). Its focal point is at 13.7 m above the ground surface. The sizes of the Field Of View (FOV) for the different incidence angles between 20° and 60°, are indicated in Table 1 and they are plotted in Fig. 1. In routine mode, LEWIS monitors brightness temperature of the fallow field, with a 40° incidence angle. An automatic scanning mode performs scanning of the surface at five incidence angles 60°, 50°, 40°, 30° and 20°, on both the fallow and the bare soil areas, eight times per day (e.g. every 3 h).

[1] Mention of manufacturers is for the convenience of the reader only and implies no endorsement on the part of the authors.

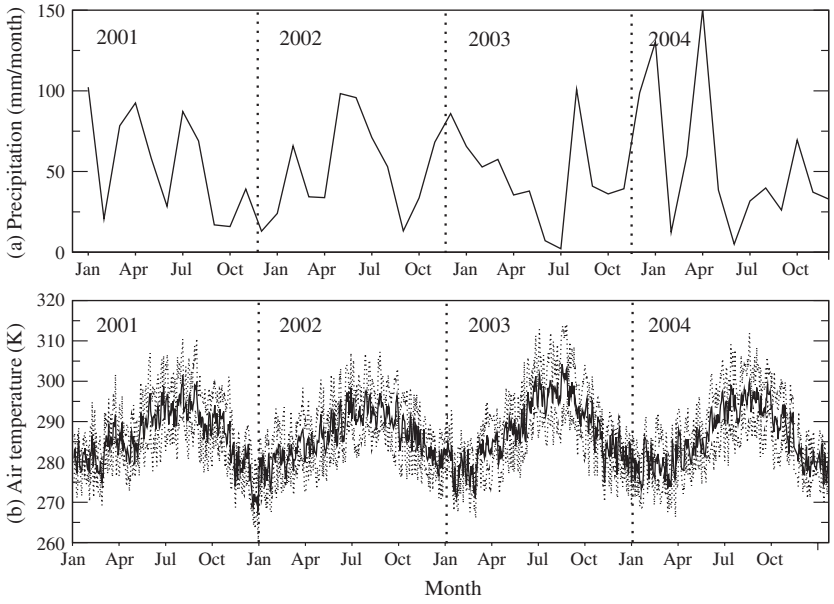

Fig. 3. 2001–2004 annual cycles of (a) monthly mean precipitation (mm/month) and (b) daily mean air temperature at 2 m (in K). Dotted lines on the bottom panel indicate minimum and maximum daily temperatures.

Within the context of the development and validation of new instruments, LEWIS measurements were used to test and validate the MARMOTTE (MAtriel Radiométrique Micro-Ondes de TTErrain) radiometer (Cohard et al., 2005; Kerr et al., 1992) in autumn 2005, as indicated in the experiment calendar (Fig. 2). However, these test results are not shown in this paper as this study focuses on 2003–2004 results.

2.3. Visible to infrared remote sensing

Two radiancemeters were installed in July, 2003, at the top of the structure. One measures the incoming solar radiation and the other the upward luminance at a 40° incidence angle over the fallow field. These two radiancemeters allow the determination of the surface reflectances at five frequencies from the visible to the near infrared and the thermal infrared (Fig. 1). The surface reflectances permit the computation of vegetation indexes such as the NDVI (Normalized Vegetation Difference Index), which is shown to be related to the LAI and is well suited to characterize the vegetation dynamics (Reed et al., 1994).

Two pyrometers has been also installed on the structure in order to monitor the thermal emission of both the bare soil and the fallow area at a 40° incidence angle since July, 2003.

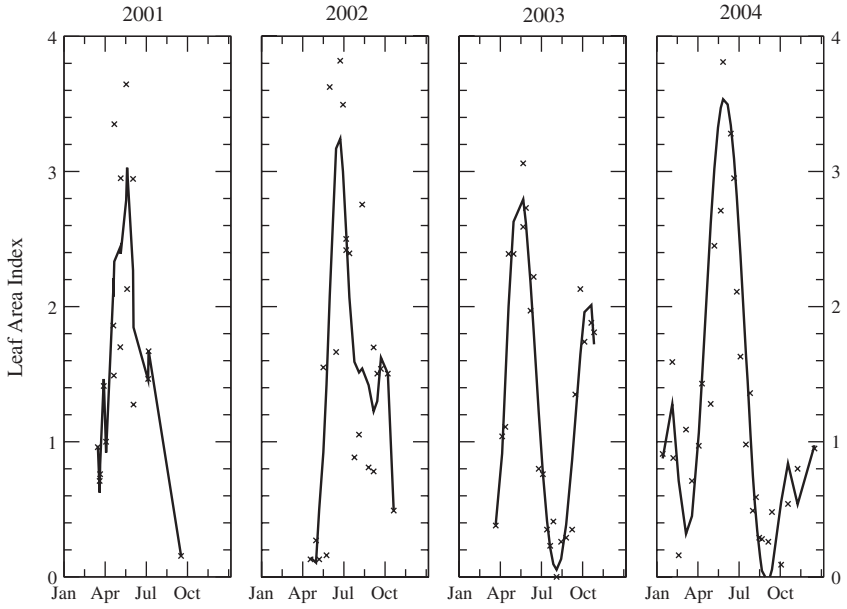

Fig. 4. Annual cycles of the vegetation Leaf Area Index (LAI) as measured (cross) in 2001, 2002, 2003 and 2004 for the SMOSREX experiment and interpolated (solid line).

In addition to these routine measurements, specific measurements were performed from November, 2004, to June, 2005, with the OWS (Optical Wetness Sensor) provided by the Free University of Amsterdam. This two-frequency active sensor (wavelength 1700 and 1930 nm) is designed to measure external vegetation water content, and it has been shown to be suitable for dew deposition measurements (De Jeu et al., 2005, 2004).

3. SMOSREX results

SMOSREX results are presented in this section. They focus on the new possibilities offered by the long term component of SMOSREX to observe, at the SMOS L-band frequency combined with multi-spectral observations, various processes from diurnal to annual and inter-annual time scales. First, the vegetation water content variability is analyzed in relation to the multi-spectral remote sensing. Then, results for both the fallow area and the bare soil are analyzed and compared from the diurnal scale to the annual scale.

3.1. Variability of vegetation water content and multi-spectral remote sensing

The two-year (2003–2004) time evolution of the measured vegetation water content is depicted in Fig. 5. The biomass internal water content is characterized by a seasonal scale dynamics and it reaches its maximum in spring, when vegetation is well developed. In contrast, dead plant material accumulated on the ground (the mulch layer) is able to absorb a large amount of water and its water content is strongly related to each individual precipitation event. Accordingly, it shows a larger temporal variability.

The vegetation water content contributes to the microwave emission of the surface. It also attenuates the emission of the soil and it attenuates its own emission (Jackson & Schmugge, 1991; Ulaby et al., 1986; Wigneron et al., 1995). The vegetation transmissivity γ is a critical variable which characterizes the vegetation effect on the microwave emission of the surface. It is expressed as a function of the vegetation optical depth, τ, and the incidence angle θ:

$$\gamma = e^{-\tau/(\cos\theta)}. \quad (1)$$

The vegetation optical depth τ is related to Vegetation Water Content (VWC) through the linear relationship:

$$\tau = b.\mathrm{VWC} \quad (2)$$

where b is a vegetation type and frequency dependent parameter (Jackson & Schmugge, 1991; Van de Griend & Wigneron, in press; Wigneron et al., in press). For satellite remote sensing applications, relationships are used between the vegetation optical depth and the remotely sensed vegetation characteristics, such as LAI from NDVI (Pellarin et al., 2003; Van de Griend & Wigneron, in press). The top panel in Fig. 6 shows the relationship obtained for the SMOSREX natural grass between the VWC and the LAI for 2003 and 2004. Two relations are established between LAI and either the total VWC, including mulch and standing biomass, or the green VWC when only standing biomass is considered. Correlation coefficients (R^2) are, respectively, 0.94 and 0.81, indicating a much higher correlation of LAI with green VWC than with total VWC. Although slopes are similar for both relationships, higher VWC is measured for the total vegetation due to the water content in the mulch layer. The scatter in the relation between VWC and LAI, when all the vegetation is considered, is clearly larger. This scatter is due to the higher variability of the total vegetation water content, due to interception of water by the mulch layer, as shown in the Fig. 5. The bottom panel in Fig. 6 shows that the LAI of the SMOSREX natural grass can be estimated with a good confidence level from space-borne remotely sensed NDVI (SPOT HRV) as well as from local radiancemeters. A very good agreement between satellite and local NDVI ($R^2 = 0.948$ for 2003) is also found (not shown). The multiple correspondence that we show between (i) the vegetation optical depth and the vegetation water content (Eq. (2)), (ii) the vegetation water content and the LAI (Fig. 6, top), and (iii) the LAI and the NDVI (Fig. 6, bottom), supports the relevance of building a suitable multi-spectral assimilation of remote sensed data in land surface models. SMOSREX provides a unique data set to investigate this issue (Muñoz Sabater et al., 2004).

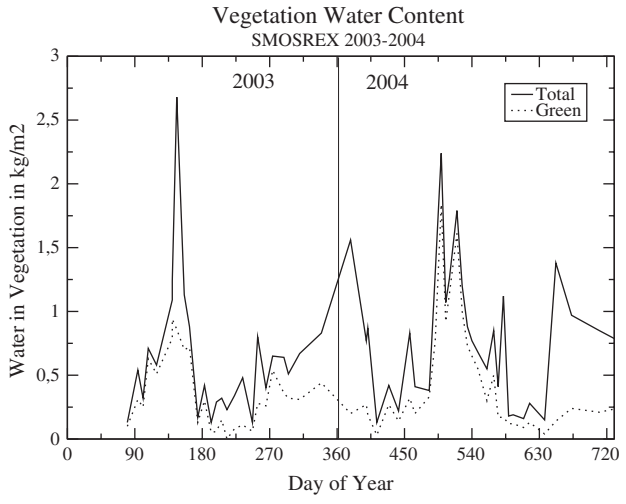

Fig. 5. Two-year dynamics of the vegetation water content measured from manual measurements of biomass and mulch. The solid line shows the total vegetation layer water content (biomass plus mulch), while the dotted line shows the biomass water content.

3.2. Effect of rainfall on the microwave emission of bare soil and natural grass

The Polarization Ratio (PR) index is used here to study the soil moisture and the vegetation water content dynamics from measured dual polarized brightness temperatures. PR is expressed as:

$$\mathrm{PR} = \frac{\mathrm{TB_v} - \mathrm{TB_h}}{\mathrm{TB_v} + \mathrm{TB_h}} \quad (3)$$

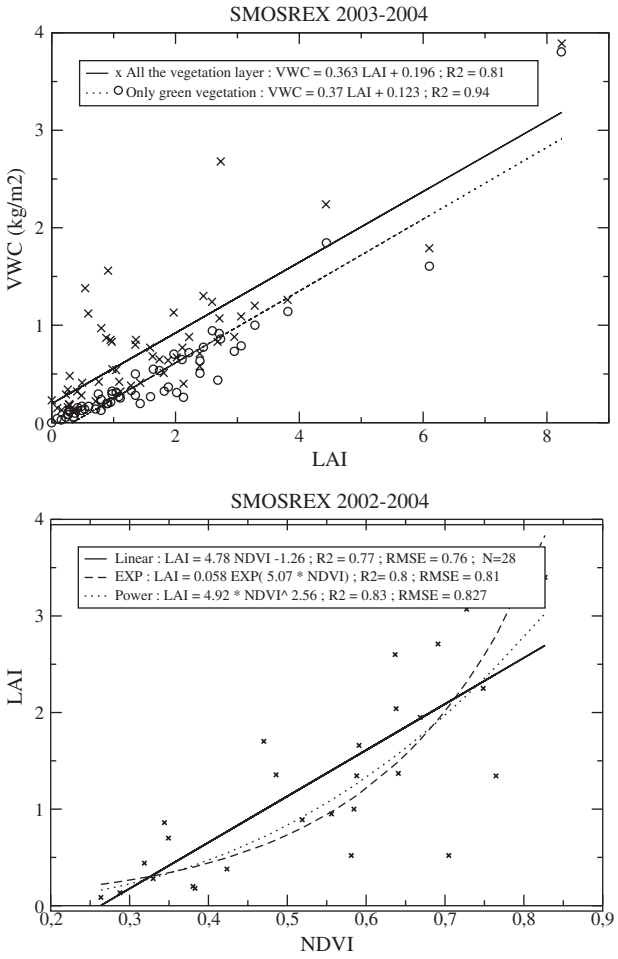

Fig. 6. Top panel: the relationship between the vegetation water content (VWC) and leaf area index (LAI) obtained for the SMOSREX fallow in 2003 and 2004. Bottom panel: relation between LAI measurements and remotely sensed NDVI (SPOT HRV, after atmospheric corrections, at 10 m resolution, over the SMOSREX field site).

where TB_v and TB_h are brightness temperatures at vertical and horizontal polarization, respectively. The PR permits the removal of temperature effects through a normalization, and it is thus mainly related to soil moisture and vegetation water content (Kerr & Njoku, 1990; Njoku et al., 2003; Owe et al., 2001).

Rainfall has a strong impact on the observed brightness temperature at the L-band. In order to illustrate this, Fig. 7 shows the impact of rainfall on the signal for a 40° incidence angle, in April, 2003, for a period where two precipitation events were monitored. Rainfall leads to a soil moisture increase for both the fallow and the bare soil. Over the bare soil, this results in a decrease of brightness temperature. This effect is stronger at the horizontal than the vertical polarization (as shown in Fig. 8 for different angles in May, 2003), leading to a positive correlation between the soil moisture and the polarization ratio. In contrast, the brightness temperature shows a lower sensitivity for fallow area after rainfall events, even showing an increase of the vegetation contribution to the signal. This lack of sensitivity for natural grass was already observed by Schmugge et al. (1988) for unburned surfaces for a few week time period. The authors explained this feature as being due to the role of the microwave absorption of the wet mulch layer (Schmugge et al., 1988). This result is confirmed here, and the thick mulch layer of SMOSREX allows one to go a step further, showing that the vegetation emission increases after a rainfall event. This shows that the water content variations of the mulch layer, related to precipitation occurrence and intensity, significantly affect the microwave emission of the surface.

This result is emphasized when we consider multi-angular measurements. Fig. 8 depicts the angular dependency of brightness temperature and PR before rain (23 May 2003, top panel), and after rain (26 May 2003, middle panel) after a sequence of 2 rainy days corresponding to 15 mm of precipitation. According to the temporal evolution plotted on Fig. 7, Fig. 8 shows that the rain effect on TBh and PR is opposite for the fallow and the bare soil areas. The increase of vegetation emission after the rainfall event is larger at a higher incidence angle.

3.3. Role of the diurnal cycle in microwave emission

Fig. 9 presents the PR as obtained from LEWIS measurements for a 40° incidence angle, together with vegetation water content measurements at different hours on the 20th of May, 2003. Over the bare soil, the PR diurnal cycle indicates soil drying during the day that leads to minimum values of soil moisture at the end of the afternoon. Over the fallow field, the diurnal cycle of the microwave signal is counter-phased with that of the bare soil due to the fact that (i) VWC dynamic is phased with that of the surface soil moisture on the bare soil at the diurnal scale, and (ii) VWC attenuates the soil emission and contributes to the global emission. The analysis of the long term time series of SMOSREX L-band measurements shows that the microwave emission of the surface typically depicts a diurnal cycle for days without rain. Accordingly, the VWC diurnal cycle includes internal and external (dew deposition) water content variations. The systematic presence of diurnal cycles for both the fallow area and the bare soil shows both that (i) the quantification of the variations of total vegetation water content at the diurnal scale and (ii) the effect of these diurnal variations on L-band measurements are important issues for passive microwave remote sensing.

3.4. Soil freezing processes and effect on L-band emission

Although slight soil freezing events occurred in February 2003 and 2004, they occurred only during a few hours during the night. A longer soil freezing period was observed in late January 2005 that lasted several days. These data are used here to illustrate the soil freezing effect on TB_h and PR. The top right panel of Fig. 10 shows that the air temperature decrease leads to bare soil temperature (at 1 cm depth) below 0 °C (273.15 K) for more than four days in a row from 25 to 29 January, with a minimum soil temperature of 266.3 K on January 28th. In contrast, the temperature of the soil for the

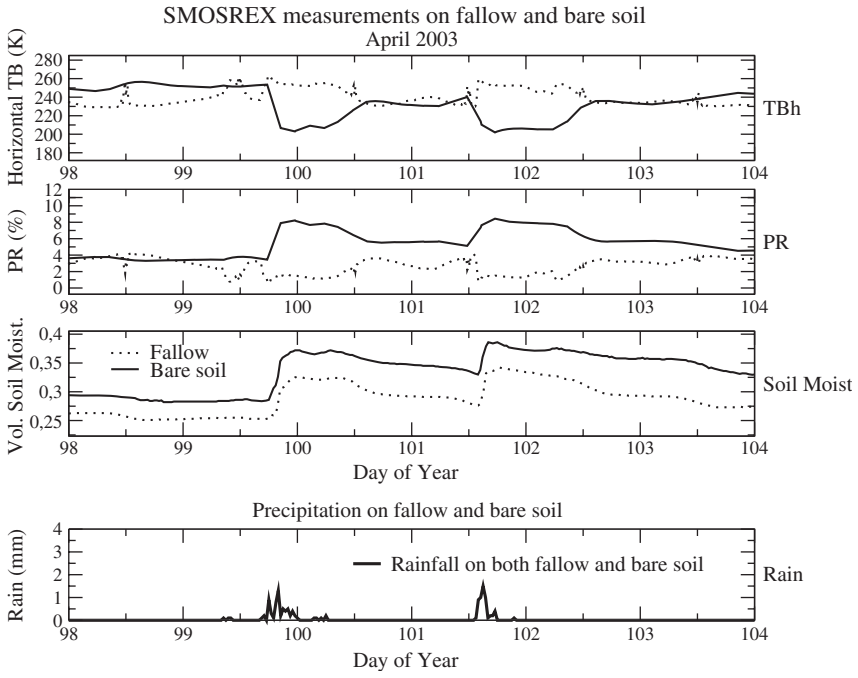

Fig. 7. Brightness temperature at horizontal polarization and PR (in %) for a 40° incidence angle, and soil moisture observed over both the fallow (dotted line) and the bare soil (solid line) plots in April 2003. Bottom panel shows the precipitation events in mm at a 30 min temporal resolution.

fallow area remains above 0 °C for the whole period, thereby avoiding freezing of the soil underneath the vegetation cover. This result is explained by the relative isolating role of the vegetation layer that is able to prevent or delay the freezing of the underlying soil.

Over the bare soil, the observed brightness temperature (top left) strongly increases as the soil liquid water content decreases due to freezing (bottom left). As shown by Hallikainen et al. (1985), this is explained by the strong influence of soil freezing on the soil dielectric permittivity whose the real part is close to 5 for frozen soils (Hallikainen et al., 1985). The PR shows a good qualitative agreement with soil moisture (bottom left panel), with a correlation $R^2=0.785$ despite the rather large scatter (rmse=3.335%, bottom right panel). Over the fallow field, the decrease of air temperature leads to vegetation freezing which is confirmed by thermal infrared temperatures that are very similar for the bare soil and the fallow area (not shown). Vegetation freezing is expected to decrease the vegetation contribution and attenuation, and to increase the soil contribution. This behavior is depicted in Fig. 10 (top left panel), where we observe a slight decrease in the horizontal brightness temperature associated with freezing events.

The effect of soil freezing on microwave emission has already been observed and is taken into account in L-band emission models (Hallikainen et al., 1985; Pellarin et al., 2003; Schwank et al., 2004). The new evidence presented here shows however that, for identical meteorological conditions and very similar thermal infra-red temperatures of the surface, the surface freezing leads to completely different effects on microwave emission depending on the vegetation cover. The vertical profile of temperature in the vegetation layer influences the occurrence of soil freezing below. The subsequent heterogeneities in soil freezing may be important at the SMOS satellite pixel size (50 km × 50 km) where mixed land cover types are considered. This new result suggests investigating the soil and vegetation temperature effects in the representation of the sub-pixel spatial variability in inversion algorithms, whenever freezing conditions are likely to occur.

3.5. Long term processes and related L-band emission

In contrast to previous field experiments using passive microwave radiometers (Choudhury et al., 1979; De Jeu et al., 2004; Eagleman & Lin, 1976; Schneeberger et al., 2004; Wang & Choudhury, 1981; Wigneron et al., 2002, 1996, 2004), which were limited to a few months at most, SMOSREX for the first time permits the observation of the long term features of L-band emission. Fig. 11 shows the annual cycle of PR with the surface volumetric soil moisture on both fallow and bare soil fields in 2003. The seasonal trend in soil moisture decrease, observed in spring (from DoY 60 to 210), produces a seasonal decrease of the PR. In fall, the soil moisture seasonal increase leads to an observed increase in PR from August to November, and the annual cycle of PR is in a very good agreement with the soil moisture annual cycle. However, from February to July the bare soil was occasionally affected by sparse growing grass. Although it was systematically removed, the discontinuous presence of sparse short vegetation might have a slight influence on the signal that must be accounted for in quantitative studies. The good agreement between the PR and the surface soil moisture is thus quantified for a longer time period (19 months), by the scatter plot shown in Fig.

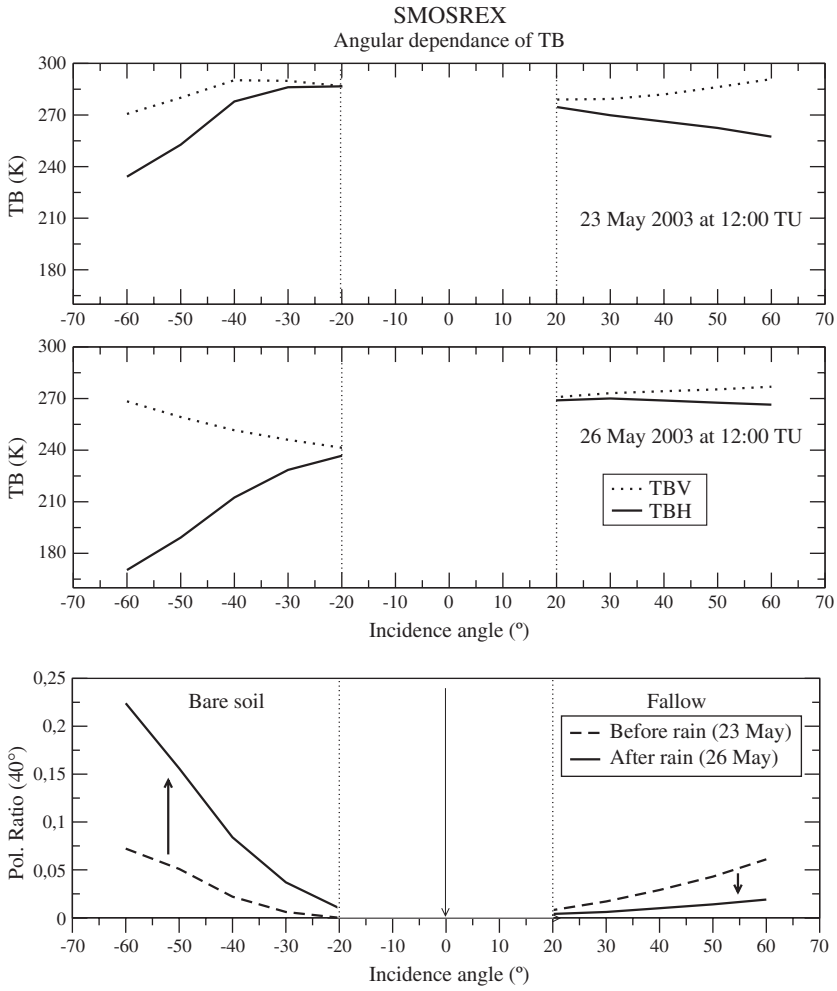

Fig. 8. Angular signature of the microwave signal on fallow and bare soil. Negative (−60° to −20°) and positive (20° to 60°) incidence angles correspond to bare soil (left) and fallow (right) respectively.

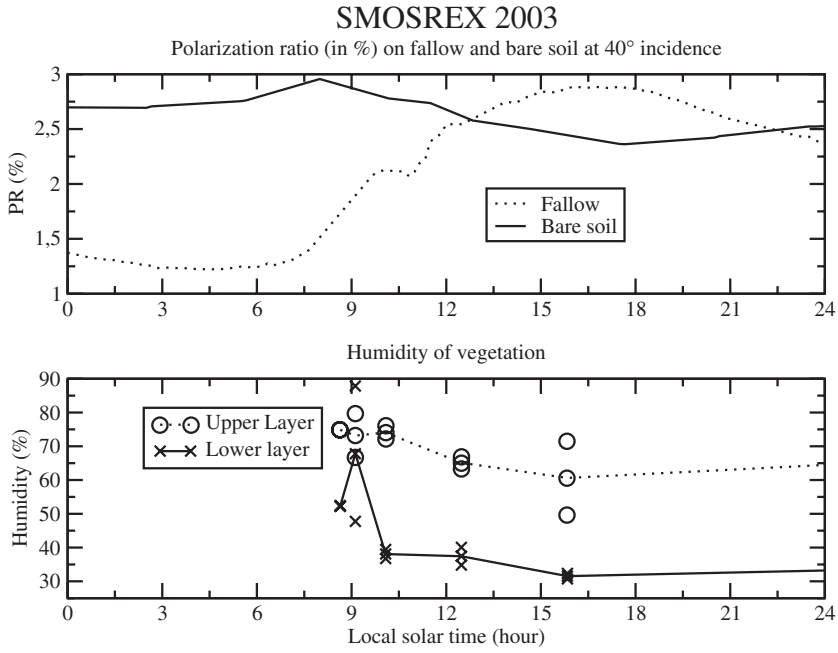

Fig. 9. Diurnal cycle of the microwave signal (PR in %) as observed for the fallow and the bare soil plots on Day of Year (DoY) 140 (20th of May) in 2003. Manual measurements of upper and lower vegetation water content.

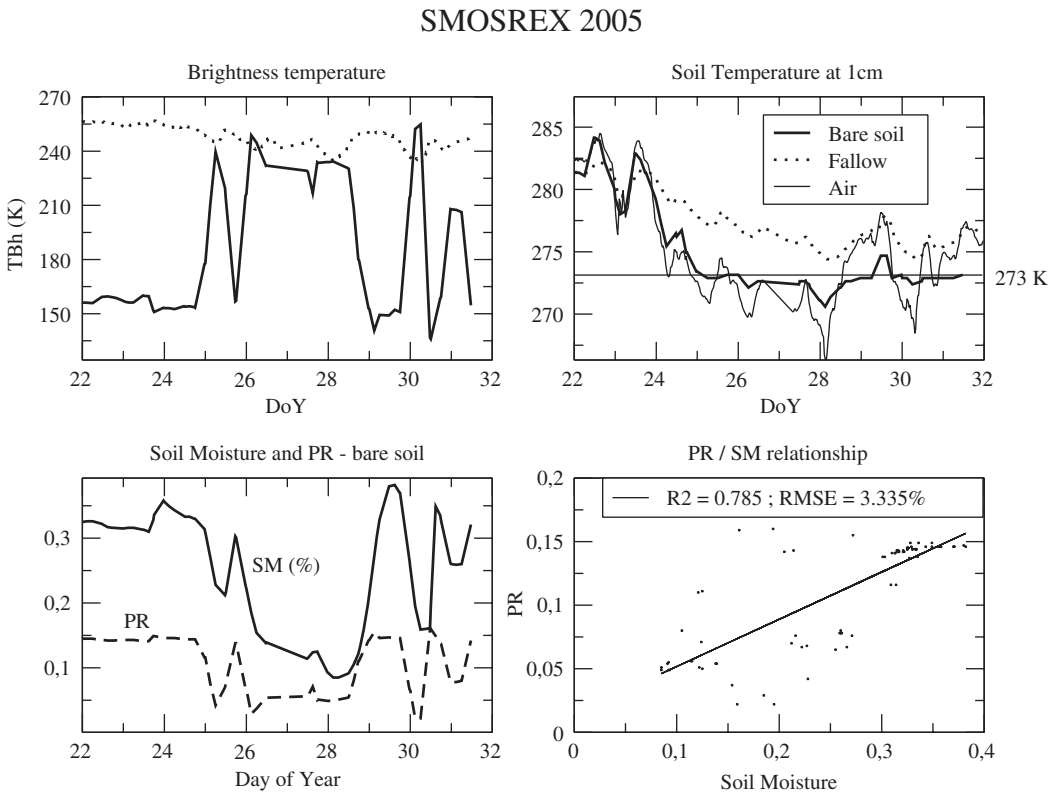

Fig. 10. Freezing events in January 2005: L-band brightness temperature at horizontal polarization as observed by LEWIS (top left) on bare (solid line) soil and fallow (dotted line). The top right panel depicts the soil temperature at 1 cm depth on both plots as well as air temperature. Bottom panel shows measurements over bare soil area. The bottom left panel shows the surface soil moisture dynamics for the same period together with PR. Bottom right is the scatter plot of PR versus soil moisture.

12 for the entire data set over absolutely bare soil from August, 2003, to February, 2005, (providing a total of 2707 values). Keeping in mind that long term data set considered here includes specific events such as freezing, or soil roughness modifications, as well as a strong annual cycle of both soil moisture and atmospheric conditions, the good correlation obtained (R^2=88.1%) is particularly noteworthy. Most of the scatter is related to soil freezing (Fig. 10) for

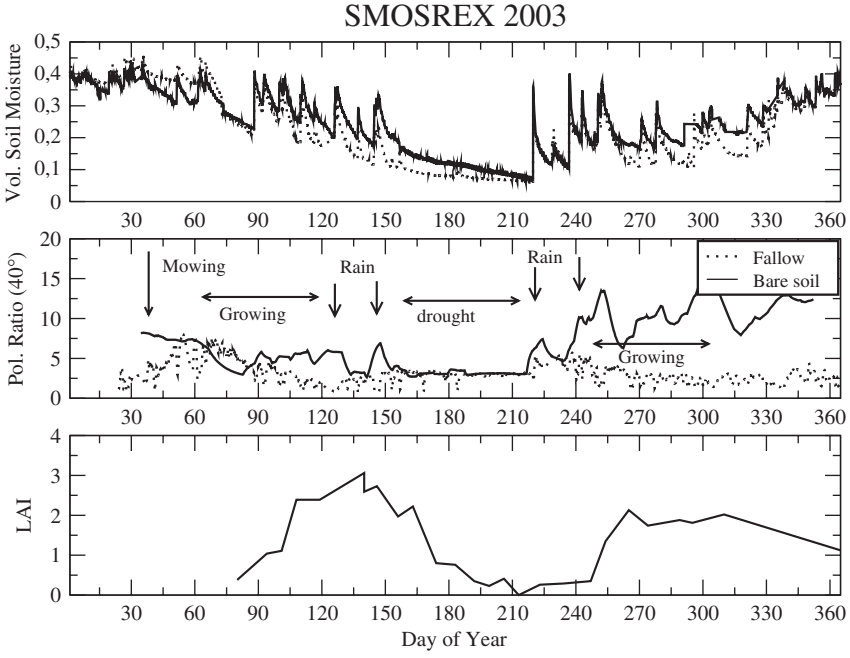

Fig. 11. Annual cycles of the soil moisture, the microwave polarization ratio (in %) at 40° on both fallow and bare soil areas. The bottom panel shows the measured LAI for the fallow area.

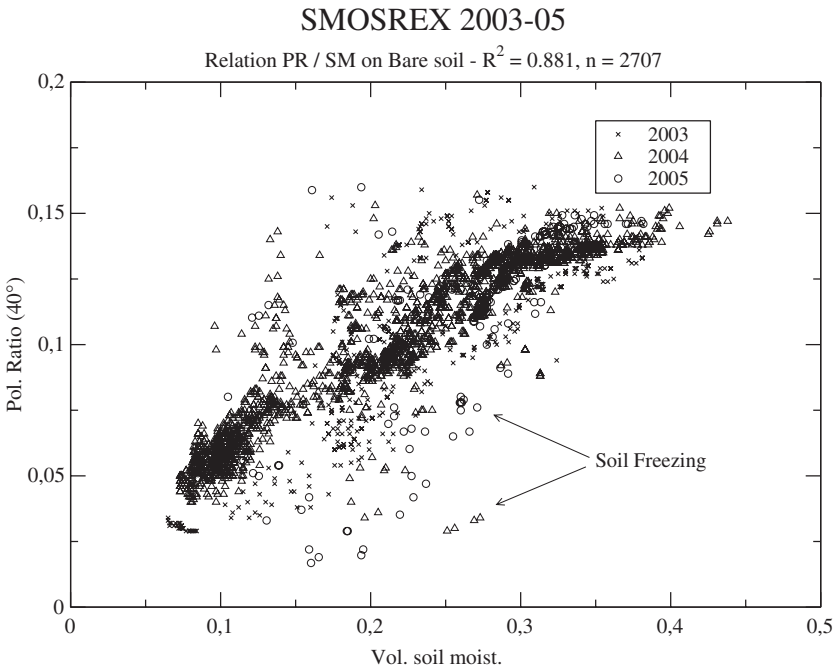

Fig. 12. Relation between the PR obtained from LEWIS measurements for a 40° incidence angle, and surface soil moisture for the bare soil. A data set of 19 months is considered, from August 2003 to February 2005, including precipitation and soil freezing events as well as soil roughness and density modifications.

lower values of PR, and soil roughness modifications (ploughing in November, 2003, and long term evolution of soil roughness). In particular, the long time series provided by SMOSREX permits the quantitative investigation of the stability of the relation between the dielectric roughness and the soil moisture for seasonal to inter-annual periods. To a smaller extent, part of the scatter is explained by the sensitivity of the soil dielectric permittivity to temperature. More details are provided in Escorihuela et al. (submitted for publication). Long term data set provided by SMOSREX also permits the validation of effective temperature parameterizations for long term time periods (de Rosnay et al., in press).

Over the fallow, it is clearly shown in Fig. 11 that the relation between soil moisture and the microwave signal is much more complex. The obtained correlation between both signals is almost non-existent ($R^2 = 0.04$) when the whole data set is considered from January 2003 to February 2005. As pointed out in previous sections for shorter temporal scales, this confirms that a simple correlation approach is not suitable to retrieve soil moisture under the vegetation canopy from microwave radiometry (Aires et al., 2005). However high temporal resolution and long time series of both radiometric and ground data SMOSREX measurements make it possible to investigate the modeling approaches required to retrieve soil moisture underneath the vegetation.

During March and April, the vegetation growth, illustrated by the LAI annual cycle (Fig. 11 bottom panel) corresponds to an increase of the vegetation water content following the relationship given in Fig. 6 (top panel). At the same time, the underlying soil undergoes a seasonal decrease in soil moisture. These opposite trends in the water content dynamics in the soil and the vegetation reservoirs result from the seasonal soil–vegetation–atmosphere interaction processes. Both lead to decreased values of PR over fallow. During summer, the heat-wave of 2003 is correlated with an absence of biomass for the fallow plot and very low soil moisture content. This explains why the PR is the same for both the fallow and the bare soil during this period. At the end of the summer, the vegetation starts to grow again after the first summer precipitation events occurred in August, in conjunction with a soil moisture increase. In contrast to spring, water content increases in both vegetation and underlying soil reservoirs. Due to opposite effect on the dynamics of the microwave signal, the contribution of the soil–vegetation system to the L-band signal is particularly intricate in fall. The PR undergoes a slight decrease in fall, indicating that vegetation water content dominates the temporal dynamics of L-band microwave emission of the surface. Combined approaches using temporal dynamics as well as angular dynamics and multi-polarized information are promising; they are investigated in SMOSREX in order to address soil moisture retrieval over vegetation covered surfaces (Saleh et al., in press; Wigneron et al., 2004).

4. Conclusion

This paper presents the SMOSREX field experiment which is dedicated to soil moisture and remote sensing measurements. SMOSREX began in 2001 with ground measurements. For the 2003–2005 period, multi-spectral remote sensing measurements were performed from the visible to the thermal infrared and L-band, by instruments placed on top of a 15 m high scaffolding. The first innovative results of L-band emission are

shown for two different surface types: a bare soil and a natural grass at different temporal scales.

At the diurnal scale, the brightness temperature dynamics is shown to be counter-phased for the bare soil and the fallow area. This is explained by the slight diurnal temporal evolution of both vegetation water content (including internal and external water content) and surface bare soil moisture. At the precipitation event scale, the vegetation water content and its related attenuation increase. This leads to opposite dynamics of L-band surface emission for the bare soil and the vegetation. At the annual scale, features of soil moisture dynamics are related to seasonal precipitation. As a consequence, the microwave signal for bare soil is linked to the seasonal trends in precipitation. For the first time, the suitability for long time periods of the relationship between polarization ratio and bare soil moisture is shown (for a 19 month period) with a 0.88 correlation coefficient. The suitability for long time period of this relation is noteworthy, given the large range of weather and soil conditions encountered. In contrast, vegetation water content dynamics are shown to be governed by both the seasonal vegetation phenology and the occurrence of precipitation events that increases the water content. This gives a much more complex microwave signature for the fallow area than on bare soil, at the annual temporal scale. It is shown that on fallow area, a direct correlation between soil moisture and polarization ratio ($R^2=0.04$) is not suitable for soil moisture retrieval. SMOSREX also permits the study of the freezing effect on both bare soil and fallow. It is shown that soil freezing occurrence is affected by the presence of vegetation. Thus, the influence of freezing on the microwave emission of the surface may be particularly important for satellite applications where mixed pixels are considered.

SMOSREX is the first long term field experiment for L-band and multi-spectral remote sensing of the surface. SMOSREX opens the possibility for many investigations in the field of microwave radiometry (soil roughness, effect of rainfall (Saleh et al., 2006), soil moisture retrieval, effective temperature), as well as in the field of land surface process modeling and understanding through land data assimilation systems developments. Ongoing and future SMOSREX related studies will be devoted to investigate these issues.

Acknowledgments

The authors thank Tom Schmugge for assistance in reviewing the text and three anonymous reviewers for their helpful comments. This work was funded by Programme National de Télédétection Spatiale and Terre Océan Surface Continentales et Atmosphère and by participants to the experiment, CESBIO, Météo France/CNRM, INRA, and ONERA.

References

Aires, F., Prigent, C., & Rossow, W. (2005). Sensitivity of satellite microwave and infrared observations to soil moisture at a global scale: 2. Global statistical relationships. *Journal of Geophysical Research*, *110*, D11103, doi:10.1029/2004JD005094.

Bindlish, R., Jackson, T. J., Gasiewski, A., Klein, M., & Njoku, E. (in press). Polarimetric scanning radiometer C and X band microwave observations during SMEX02, *Remote Sensing of the Environment*.

Calvet, J. -C., Bessemoulin, P., Noilhan, J., Berne, C., Braud, I., Courault, D., et al. (1999). Murex: A land-surface field experiment to study the annual cycle of the energy and water budgets. *Annales Geophysicae*, *17*, 838–854.

Choudhury, B. J., Schmugge, T. J., Chang, A., & Newton, R. W. (1979). Effect of surface roughness on the microwave emission from soils. *Journal of Geophysical Research*, *84*(9), 5699–5706.

Cohard, J. M., Mercier, B., Laurent, J. P., Pellarin, T., Kerr, Y., & de Rosnay, P. (2005). *Développement de radiomètres microondes pour la mesure des teneurs en eau de surface: mise au point et premiers tests d'un radiomètre à 4.3 Ghz.* ECCO-PNRH colloque.

De Jeu, R., Heusinkveld, B., Groot, S., de Rosnay, P., Holmes, T., & Owe, M. (2005). The effect of dew on passive L-band microwave observations. *EGU 2nd general assembly; Vienna (Austria), 24–29 April.*

De Jeu, R., Heusinkveld, B., Vugts, H., Holmes, T., & Owe, M. (2004). Remote sensing techniques to measure dew: The detection of canopy water with an L-band passive microwave radiometer and a spectral reflectance sensor. *SPIE proceeding*.

De Jeu, R., Holmes, T., & Owe, M. (2004). Deriving land surface parameters from three different vegetated sites with the Elbara 1.4-Ghz passive microwave radiometer. *Proceedings of SPIE*, *vol. 5232*.

de Rosnay, P., Wigneron, J. -P., Holmes T., & Calvet, J. -C. (in press). Parameterizations of the effective temperature for L-band radiometry. Inter-comparison and long term validation with SMOSREX field experiment. In C. Mätzler (Ed.), *Radiative Transfer Models for Microwave Radiometry.* Institution of Electrical Engineers, Stevenage, UK.

Eagleman, J. R., & Lin, W. C. (1976). Remote sensing of soil moisture by a 21-cm passive radiometer. *Journal of Geophysical Research*, *84*(9), 3660–3666.

Entekhabi, D., Asrar, G. R., Betts, K. J., Beven, A. K., Bras, R. L., Duffy, C. J., et al. (1999). An agenda for land surface hydrology research and a call for the second international hydrological decade. *Bulletin of the American Meteorological Society*, *10*, 2043–2058.

Entekhabi, D., Njoku, E. G., Houser, P., Spencer, M., Doiron, T., Kim, Y., et al. (2004). The Hydrosphere State (Hydros) Satellite Mission: An Earth System Pathfinder for Global Mapping of Soil Moisture and Land Freeze/Thaw. *IEEE Transactions on Geoscience and Remote Sensing*, *42*(10), 2184–2195.

Escorihuela, M. J., de Rosnay, P., Kerr, Y. (submitted for publication). Temperature dependency of bound water spectral parameters and its influence in soil moisture measurements, *Water Resources Research*.

Hallikainen, M. T., Ulaby, F., & Dobson, M. (1985). Microwave dielectric behaviour of wet soil: Part 1. Empirical models and experimental observations. *IEEE Transactions on Geoscience and Remote Sensing*, *23* (1), 25–33.

Jackson, T. J., LeVine, D., Hsu, A., Oldak, A., Starks, P., Swift, C., et al. (1999). Soil moisture mapping at regional scales using microwave radiometry: The southern great plains hydrology experiment. *IEEE Transactions on Geoscience and Remote Sensing*, *37*, 2136–2150.

Jackson, T. J., Le Vine, D., Swift, C., & Schmugge, T. J. (1995). Large scale mapping of soil moisture using the ESTAR passive microwave radiometer. *Remote Sensing of the Environment*, *53*, 27–37.

Jackson, T., & Schmugge, T. (1991). Vegetation effects on the microwave emission of soils. *Remote Sensing of the Environment*, *36*, 203–212.

Kerr, Y., & Njoku, E. (1990). A semi empirical model for interpreting microwave emission from semiarid surfaces as seen from space. *IEEE Transactions on Geoscience and Remote Sensing*, *28*, 384–393.

Kerr, Y., Leroy, Y., Laguerre, L., Bertuzzi, P., & Van de Velde, J. C. (1992). Marmotte: A portable field microwave radiometer. *Presented at Specialists meeting on microwave radiometry.* Boulder, Co, USA.

Kerr, Y., Waldteufel, P., Wigneron, J. -P., Martinuzzi, J. -M., Font, J., & Berger, M. (2001). Soil moisture retrieval from space: The soil moisture and ocean salinity (SMOS) mission. *IEEE Transactions on Geoscience and Remote Sensing*, *39*(8), 1729–1735.

Koster, R. D., Dirmeyer, P., Guo, Z., Bonan, G., Cox, P., Gordon, C., et al. (2004). Regions of strong coupling between soil moisture and precipitation. *Sciences*, *305*.

Lemaître, F., Poussière, J. C., Kerr, Y., Dejus, M., Durbe, R., de Rosnay, P., et al. (2004). Design and test of the ground based L-band radiometer for Estimating Water In Soils (LEWIS). *IEEE Transactions on Geoscience and Remote Sensing*, *42*(8), 1666–1676.

Muñoz Sabater, J., Calvet, J. C., & de Rosnay, P. (2004). On the assimilation of multispectral remote sensing data in a SVAT model. *(IGARSS'04), 20–24 Sept, Anchorage, Alaska, USA*.

Njoku, E., Jackson, T., Lakshmi, V., Chan, T., & Nghiem, S. (2003). Soil moisture retrieval from AMSR-E. *IEEE Transactions on Geoscience and Remote Sensing*, *41*(2), 215–229.

Owe, M., De Jeu, R., & Walker, J. (2001). A methodology for surface soil moisture and vegetation optical depth retrieval using the microwave polarization difference index. *IEEE Transactions on Geoscience and Remote Sensing*, *39*(8).

Pellarin, T., Wigneron, J. -P., & Waldteufel, P. (2003). Global soil moisture retrieval from a synthetic L-band brightness temperature data set. *Journal of Geophysical Research*, *108*(D12), doi:10.1029/2002JD003086.

Reed, B., Brown, J., van der Zee, D., Loveland, T., Merchant, J., & O (1994). Vegetation effects on the microwave emission of soils. *Journal of Vegetation Science*, *5*, 703–714.

Saleh, K., Wigneron, J. -P., de Rosnay, P., Calvet, J. -C., Escorihuela, M. J., Kerr, Y., & Waldteufel, P. (2006). Impact of rain interception by vegetation and mulch on the L-band emission of natural grass. *Remote Sensing the Environment*, *101*(1), 127–139.

Saleh, K., Wigneron, J. -P., de Rosnay, P., Calvet, J. -C., & Kerr, Y. (in press). Semi-empirical regressions at L-band applied to surface retrievals over grass, *Remote Sensing of the Environment*.

Schmugge, T. J., Jackson, T. J., Kustas, W. P., & Wang, J. R. (1992). Passive microwave remote sensing of soil moisture: results from HAPEX, FIFE and MONSOON 90. *ISPRS Journal of Photogrammetry and Remote Sensing*, *47*, 127–143.

Schmugge, T. J., Wang, J. R., & Asrar, G. (1988). Results from the Push Broom Microwave Radiometer Flights over the Konza Prairie in 1985. *IEEE Transactions on Geoscience and Remote Sensing*, *26*(5), 590–596.

Schneeberger, K., Stamm, C., Mätzler, C., & Flühler, H. (2004). Groundbased dual-frequency radiometry of bare soil at high temporal resolution. *IEEE Transactions on Geoscience and Remote Sensing*, 588–595.

Schwank, M., Stähli, M., Wydler, H., Leuenberger, J., Mätzler, C., & Hannes, F. (2004). Microwave L-band emission of freezing soil. Microwave dielectric behaviour of wet soil: Part I. Empirical models and experimental observations. *IEEE Transactions on Geoscience and Remote Sensing*, *23* (1), 1252–1261.

Ulaby, F., Moore, R., & Fung, A. (1982). *Microwave remote sensing: active and passive. Radar remote sensing and surface scattering and emission theory*, *vol. II.* Addison-Wesley Publishing company.

Ulaby, F., Moore, R., & Fung, A. (1986). *Microwave remote sensing: active and passive. From theory to application*, *vol. III.* Dedham, MA: Artech House.

Van de Griend, A., & Wigneron, J. -P. (in press). The b-factor relating vegetation optical depth to vegetation water content. In C. Mätzler (Ed.), *Radiative Transfer Models for Microwave Radiometry.* Institution of Electrical Engineers, Stevenage, UK.

Wang, J. R. (1983). Passive microwave sensing of soil moisture content: The effects of soil bulk density and surface roughness. *Remote Sensing of the Environment*, *13*, 329–344.

Wang, J. R., & Choudhury, B. J. (1981). Remote sensing of soil moisture content over bare field at 1.4 GHz frequency. *Journal of Geophysical Research*, *86*, 5277–5282.

Wigneron, J. -P., Calvet, J. -C., de Rosnay, P., Kerr, Y., Waldteufel, P., Saleh, K., et al. (2004). Soil moisture retrievals from bi-angular L-band passive microwave observations. *IEEE Transactions on Geoscience and Remote Sensing Letter*, *1*(4), 277–281.

Wigneron, J. -P., Calvet, J. -C., & Kerr, Y. (1996). Monitoring water interception by crop fields from passive microwave observations. *Agricultural and Forest Meteorology*, *80*, 177–194.

Wigneron, J. -P., Chanzy, A., Calvet, J. -C., & Bruguier, N. (1995). A simple algorithm to retrieve soil moisture and vegetation biomass using passive microwave measurements over crop fields. *Remote Sensing of the Environment*, *51*, 331–341.

Wigneron, J. P., Chanzy, A., Calvet, J. C., Olioso, A., & Kerr, Y. (2002). Modeling approaches to assimilating L-band passive microwave observations over land surfaces. *Journal of Geophysical Research*, *107*(14), doi:10.1029/2001JD000958.

Wigneron, J. P., Parde, M., Waldteufel, P., Chanzy, A., Kerr, Y., Schmidl, S., et al. (2004). Characterizing the dependence of vegetation model parameters on crop structure, view angle and polarization. *IEEE Transactions on Geoscience and Remote Sensing*, *42*(2), 416–425.

Wigneron, J. -P., Pellarin, T., Calvet, J. -C., de Rosnay, P., & Kerr, Y. (in press). L-meb: A simple model at L-band for the continental areas — Application to the simulation of a half-degree resolution and global scale data set. In C. Mätzler (Ed.), *Radiative Transfer Models for Microwave Radiometry.* Institution of Electrical Engineers, Stevenage, UK.